Ab initio derived kinetic Monte Carlo model of H_2 desorption from Si(100)-2×1

Michelle R. Radeke and Emily A. Carter*
Department of Chemistry and Biochemistry, University of California-Los Angeles, 405 Hilgard Avenue, Los Angeles, California 90095-1569
(Received 12 August 1996)

Using an *ab initio* derived kinetic Monte Carlo model, we show that within the framework of a mechanism involving the systematic conversion of monohydrides to dihydrides and the prepairing assumption, H_2 desorption from Si(100)-2×1 via isolated dihydrides follows first-order kinetics. Our model predicts that the kinetic order is invariant with respect to coverage, temperature, and surface features (e.g., steps and defects). However, we show that the concentration of defects on the surface has a profound effect on the desorption rate constant. The dependence of the rate constant on surface quality might explain the wide range of experimental values reported for the desorption rate constant. [S0163-1829(97)06207-3]

I. INTRODUCTION

H_2 desorption from Si(100)-2×1 follows first-order kinetics,[1–5] which is unusual when contrasted with the second-order kinetics observed for H_2 desorption from Si(111)-7×7 and from metal surfaces. Since second-order kinetics are expected for a desorption mechanism which consists of hydrogen atoms diffusing randomly on a surface, recombining, and desorbing, the first-order kinetics for this process on Si(100)-2×1 must be due to the unique features of this surface. Indeed, there has been a lively discussion in the past few years over the origin of this interesting kinetic behavior.[6]

Mechanisms proposed to explain this oddity involve delocalized hydrogen diffusion followed by fast desorption, hydrogen desorption from a single silicon dimer on which the hydrogen atoms are ''prepaired,'' monohydride to dihydride isomerization to produce dihydrides (H-Si-Si-$H_{(a)}$→Si +$SiH_{2(a)}$) from which desorption occurs, and desorption via isolated dihydrides. We have previously ruled out the delocalized hydrogen mechanism and the monohydride-dihydride isomerization mechanism.[7,8] The ''prepairing'' mechanism is attractive in that it takes advantage of the unique feature on the Si(100)-2×1 surface, the dimer rows, to explain the first-order kinetics. This mechanism is based on theoretical,[9–11] and experimental[12] evidence which suggests that hydrogen atoms are prepaired on silicon dimers due to the thermodynamic preference of the prepairing configuration (H-Si-Si-H +Si-Si) over nonprepairing arrangements (H-Si-Si+H-Si-Si), and the work of D'Evelyn and co-workers[11,13] who used a simple statistical mechanical model and showed that within the prepairing assumption, desorption follows first-order kinetics.

Attractive as the prepairing mechanism may be from this point of view, previous calculations by us[7] and others[14,15] find that the activation barrier for desorption via a prepairing pathway is too high to explain the desorption kinetics measured by experiments. Our prior calculations also indicate that the prepairing mechanism is inconsistent with other kinetic and dynamic experimental observations.[7] Furthermore, recent reduced-dimensionality quantum and quasiclassical dynamical simulations on a density-functional-theory-derived potential-energy surface have demonstrated quantitative disagreement of the prepairing mechanism with experimental observations. Both the temperature dependence of H_2 adsorption probabilities and the translational energy of desorbing H_2 were inconsistent with this mechanism.[16] In our previous work, we offer a detailed explanation of why we believe desorption occurs from isolated dihydrides, a mechanism which is also supported by the theoretical calculations of Nachtigall, Jordan, and Sosa[14] and Jing and Whitten.[15] It is our purpose in the present work to investigate whether desorption via this mechanism can follow first-order kinetics as we[7,8] and others[14,15] have proposed.

A requirement for this pathway to desorption is the presence of silicon atoms with two free dangling bonds (isolated atom defects). Jing *et al.*[17] proposed that these lone silicon atoms could be created at steps. An alternative proposal by Kolasinski *et al.*[18,19] is the spontaneous formation of isolated silicon atoms from dimerized silicon atoms (Si-Si→Si+Si) which they suggest as a probable situation at the high temperatures (700–900 K) at which hydrogen desorption from Si(100)-2×1 occurs. Since the isolated silicon atoms are regenerated through desorption, only a small percentage of these atoms would be required in the isolated dihydride mechanism. Nachtigall, Jordan, and Sosa[14] suggested that lone silicon atoms could migrate throughout the Si(100)-2×1 surface (Si+Si-Si→Si-Si+Si). Furthermore, they proposed that when these isolated silicon atoms encounter a monohydride, a dihydride could be created (H-Si-Si-$H_{(a)}$+Si →Si-Si+$SiH_{2(a)}$). Since the barriers Nachtigall, Jordan, and Sosa calculated for these processes are small compared to desorption, they reasoned that there would be an equilibrium distribution of dihydrides from which hydrogen could desorb; thus, their defect migration mechanism might be able to explain the first-order kinetics.[14]

The work of D'Evelyn and co-workers[11,13] illustrated that the population of monohydrides is proportional to the hydrogen coverage, Θ(H-Si-Si-$H_{(a)}$)~Θ(H). Therefore, if monohydrides are systematically converted to dihydrides through a step such as the defect migration mechanism of Nachtigall, Jordan, and Sosa[14] then $\Theta(SiH_{2(a)})\sim\Theta$(H-Si-Si-$H_{(a)}$) and, consequently, it follows that $\Theta(SiH_{2(a)})\sim\Theta$(H). We set out to model the kinetic behavior of the isolated dihydride

mechanism for desorption within the framework of the defect migration mechanism[14] and the prepairing assumption, using an *ab initio*–derived kinetic Monte Carlo (KMC) simulation, in order to establish if such a mechanism follows a first-order dependence on $\Theta(H)$.

II. THE MODEL

A. A general kinetic Monte Carlo scheme

KMC simulations are intended to fill a gap between Monte Carlo (MC) and molecular-dynamics (MD) simulations. With MC simulations one can obtain equilibrium configurations for a large or complex system, but no dynamical information about how the system reached the equilibrium state is provided. On the other hand, with MD simulations dynamics are directly monitored, but the time scale is limited to at most a nanosecond, or less, if the system is large and requires the evaluation of a complicated potential energy expression. The premise of KMC is to relate MC steps to real time in order to simulate dynamical systems. Fichthorn and Weinberg[20] have established that a Monte Carlo simulation following the master equation (the detailed balance equation) can be related to a Poisson distribution if three criteria are met: (i) there needs to be a hierarchy of dynamical processes which satisfy detailed balance, (ii) the MC steps must be related to time correctly, and (iii) the events must be independent. In practice, this means that to perform a KMC simulation, one needs to identify the kinetic pathways to be included in the model, have some way of ranking the occurrence of these processes based on their respective time scales and of updating the time in the simulation based on MC steps, and assure that the occurrence of these events within the model is sufficiently random. Because rate constants are usually not known exactly and not all kinetic pathways can be included in the simulation, a KMC simulation is not intended to give quantitative information about the dynamics. Instead, the goal is to identify processes important to the dynamics and have an estimate of the ratio of their rate constants in order to qualitatively predict kinetic behavior.

The basic implementation of the KMC simulation[21] consists of the following loop: Step 1, an atom is chosen at random out of all of the available atoms in the system which can participate in an event; step 2, based on the environment of the atom or type of atom chosen a type of process is randomly selected; step 3, the chosen event occurs with a probability of k/k_r, where k is the rate constant of the chosen process and k_r is the fastest process possible in the model (this event always happens when chosen); step 4, after N attempted moves, where N is the number of atoms in the system which can undergo events, the time is incremented by $1/k_r$, step 5, repeat.

Because the time scale of the KMC simulation depends on $1/k_r$, in order to keep the simulation computationally feasible it is important to choose to model the interplay between processes which are on similar time scales. For instance, if k_r is on the order of $1\times10^{2}\ s^{-1}$ (i.e., a time scale of milliseconds) and the slowest process in the model has a rate constant of $1\times10^{-6}\ s^{-1}$ (i.e., a time scale of weeks), then, for every loop through the simulation the time is only updated by one millisecond and it would take an average of 100 million loops for each occurrence of the slowest event. The time consumed in each loop depends on the complexity of the logic (which is contingent on how the environment of the chosen atom is determined and the number and type of events which that atom can undergo) and on the number of atoms in the system. Since random numbers are used to pick the atom and type of move, and to determine whether a move is accepted based on its probability, in the example above, a moderately sized system of 100 atoms would require tens of billions of random numbers to be generated for each episode of the slowest event. For a simulation to be realistic, many more than one episode of each type of event should occur.

B. Determining and ranking the processes involved in hydrogen desorption from the Si(100)-2×1 surface

The main processes which are most likely to influence the kinetics of hydrogen desorption from the Si(100)-2×1 surface are hydrogen diffusion parallel and perpendicular to the dimer rows, the migration of defects, defect-induced isomerization to (H-Si-Si-$H_{(a)}$+Si→$SiH_{2(a)}$+Si-Si) and from ($SiH_{2(a)}$+Si-Si→H-Si-Si-$H_{(a)}$+Si) dihydrides, monohydride to dihydride (H-Si-Si-$H_{(a)}$→Si+$SiH_{2(a)}$), and dihydride to monohydride (Si+$SiH_{2(a)}$→H-Si-Si-$H_{(a)}$) isomerization on a single silicon dimer, and hydrogen desorption. The first column in Table I offers a pictorial summary of these processes.

A crucial process in the defect migration mechanism for desorption is the rate at which the defects convert monohydrides to dihydrides and the dihydrides revert back to monohydrides and lone silicon atoms, since in our model the dihydrides are the sites at which desorption takes place. As mentioned earlier, Nachtigall, Jordan, and Sosa[14] proposed this so-called ''defect migration'' mechanism based on their calculations for the activation energies for defect migration and defect-induced isomerization. They determined these barriers by performing single-point density-functional-theory (DFT) calculations using the Becke3LYP functional on transition state (TS) and minimum-energy structures which were geometry optimized at the local-spin-density–DFT level of theory in C_s symmetry using $Si_{16}H_{20}$ and $Si_{16}H_{18}$ clusters. Nachtigall, Jordan, and Sosa calculated activation energies[22] for forward (H-Si-Si-$H_{(a)}$+Si→$SiH_{2(a)}$+Si-Si) and reverse isomerization ($SiH_{2(a)}$+Si-Si→H-Si-Si-$H_{(a)}$+Si) to be 1.65 and 1.56 eV, respectively.[14]

Using the optimized geometries provided by Nachtigall, Jordan, and Sosa we calculated the vibrational frequencies for the minimal energy and TS structures for the defect isomerization mechanism. The vibrational frequencies were obtained from a numerical Hessian (energy second-derivative matrix) determined by finite differences of analytical gradients. Finite displacements of 0.01 Bohr were made from the optimal geometry in both a positive and negative direction leading to two times $3N$ displacements, where N is the number of symmetry unique atoms. Because of the large nature of the cluster, energy and gradient calculations were determined at the Hartree-Fock self-consistent-field (HFSCF) level.[23] Basis sets used for the silicon atoms and the adsorbate hydrogen atoms are given in Ref. 7. To make the calculation managable, a minimal 1's basis set composed of two Gaussian functions was used for the hydrogen atoms which terminate the cluster.[24] Using a minimal basis set for the terminating hydrogen atoms seems reasonable, since the

TABLE I. Summary of processes involved in H_2 desorption from Si(100)2×1.

Process	k (s^{-1}) at 800 K and source	role in model
defect migration 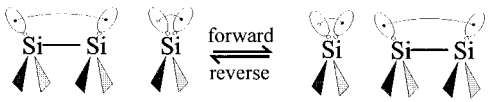	10^6 to 10^{11} DFT Ref. 14	randomize unoccupied defect population at each step
intra-row hydrogen atom diffusion 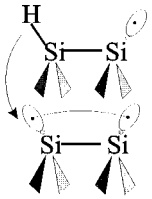	1.1×10^5 MRSDCI/MCTST Ref. 25	randomize monohydride and bare silicon dimer populations at each step
monohydride-dihydride isomerization 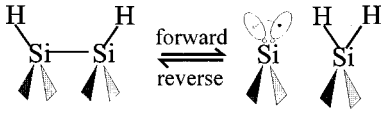	$k_{forward} = 4.8\times10^1$ $k_{reverse} = 2.0\times10^7$ MRSDCI/CASSCF Ref. 7	no role -- estimate amount of dihydrides created via this process is negligible
defect-induced isomerization 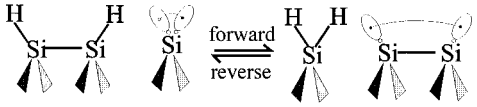	$k_{forward} = 1.0\times10^5$ $k_{reverse} = 8.0\times10^4$ DFT/HF Ref. 14/this work	$k_{forward}$ is the reference and $k_{reverse}$ is included as a possible move
hydrogen desorption (isolated dihydride pathway) 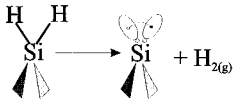	0.048 to 2.77 Experiment Ref. 1-5 9.9×10^{-4} MRSDCI/CASSCF Ref. 7	use most accurate experimental Arrhenius parameters, so that k = 0.196 s^{-1}
inter-row hydrogen atom diffusion 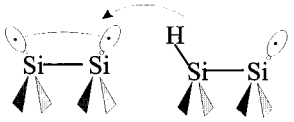	1×10^{-3} MRSDCI/MCTST Ref. 25	no role -- estimate little effect, as this process is slower than desorption
hydrogen desorption (prepairing pathway) 	4.0×10^{-8} MRSDCI/CASSCF Ref. 7	no role -- rare event

frequencies of these terminating hydrogen atoms in the TS and adsorbed structures should cancel each other out in the framework of simple transition state theory (STST) which expresses the preexponential factor, A, as the product of nonzero vibrational frequencies at the minimum-energy structure divided by the product of the real, nonzero vibrational frequencies at the TS, $A=(\Pi^{3N-6}\nu_{\min}/\Pi^{3N-7}\nu_{TS})$, where N is the number of atoms.[25] We scaled the vibrational frequencies by the conventional factor of 0.9 (HFSCF calculations are well known to yield frequencies about 10% too high) before using them in the STST formulation to determine the preexponential for isomerization (6.0×10^{14} s^{-1}) and reverse isomerization (1.2×10^{14} s^{-1}). We also used these scaled vibrational frequencies to add zero-point energy corrections to the activation barriers determined by Nachtigall, Jordan, and Sosa[14] leading to new values for the energy barriers for isomerization (1.55 eV) and reverse isomerization (1.46 eV). Using our calculated preexponentials and the corrected energy barriers in the Arrhenius equation, we predict rate constants of $k_{forward}=1.0\times10^5$ s^{-1} and $k_{reverse}=8.0\times10^4$ s^{-1}. Both forward and reverse isomerization occur on the same time scale ($\tau=1/k$) of $\tau\sim1\times10^{-5}$ s.

A preceding step essential to the defect migration mechanism, the migration of lone silicon atoms, occurs much more rapidly than defect-induced isomerization. Using the activation energy of 0.6 eV that Nachtigall, Jordan, and Sosa predicted for defect migration, along with a typical range of values for the preexponential in the Arrhenius equation (10^{10} s^{-1} and 10^{15} s^{-1}), we estimate that the rate constant for this process at 800 K is between 10^6 s^{-1} and 10^{11} s^{-1} ($\tau\cong10^{-6}$ s to 10^{-11} s). Thus, defect migration, at the temperature at which hydrogen desorption occurs, is a fast process compared to defect isomerization. Additionally, it is an extremely fast process compared to hydrogen desorption. Since

defect migration occurs too quickly to include directly in our model, we did not perform *ab initio* calculations to determine the rate constant of this process more accurately. In Sec. II C, we discuss how defect migration was incorporated into the KMC simulation.

For hydrogen desorption, the experimental values for the rate constant at 800 K range from 0.048 to 2.77 s^{-1} ($\tau=2\times10^{-1}$–4×10^{-1} s).[1–5] The most accurate estimates for the rate constant (based on reported error bars in the Arrhenius parameters) are from Höfer, Li, and Heinz[4] ($E_a=2.48\pm0.1$ eV and $A\sim2\times10^{15}$ s^{-1}), Wise *et al.*[2] ($E_a=2.51$ eV and $A\sim5.5\times10^{15}$ s^{-1}), and Flowers *et al.*[5] ($E_a=2.47$ eV and $A\sim2\times10^{15}$ s^{-1}). From these estimates, we chose Arrhenius parameters of $A=1.0\times10^{15}$ s^{-1} and $E_a=2.49$ eV, giving us a rate constant, in our model, of 0.196 s^{-1} for desorption from dihydrides at 800 K. We do not use our own *ab initio* estimate of the rate constant for desorption via the isolated dihydride pathway ($k=9.9\times10^{-4}$ s^{-1} and $\tau=1\times10^{3}$ s), as we anticipate that our calculation predicts a lower rate constant than experiment due to errors inherent to our *ab initio* approach.[7] We also do not include desorption via the prepairing pathway in our simulation since our predicted *ab initio* rate constant for this process ($k=4.0\times10^{-8}$ s^{-1} and $\tau=1\times10^{7}$ s)[7] would make the time-scale difference between defect isomerization and desorption much too large, resulting in an intractable calculation. Most importantly, we have shown that even taking into account our anticipated errors in the rate constant calculation does not make desorption through the prepairing pathway anything but an extremely rare event.[7]

Two independent theoretical calculations have identified hydrogen diffusion parallel to the silicon dimer rows (parallel or intra-row diffusion) as a much faster process than diffusion perpendicular to the silicon dimer rows (perpendicular or inter-row diffusion). Wu *et al.*[26] performed *ab initio*–derived Monte Carlo transition state theory (MCTST) calculations and determined that intra-row diffusion had a rate constant of 1.1×10^{5} s^{-1} ($\tau=9.1\times10^{-6}$ s), while inter-row diffusion had a much smaller rate constant 1×10^{-3} s^{-1} ($\tau=1\times10^{3}$ s). This is in agreement with the local-density approximation DFT calculations of Vittadini, Selloni, and Casarin[27] which did not determine rate constants, but which predicted that the activation barrier for intra-row diffusion is 0.5 eV lower than that for inter-row diffusion. Thus, in our model, we have parallel diffusion occurring more rapidly than defect isomerization, as does defect migration, and perpendicular diffusion happening on a longer time scale than desorption, making inter-row hydrogen diffusion the slowest process in our model.

The last process we have to consider is monohydride-dihydride isomerization on a single silicon dimer. In previous work,[7] we predicted *ab initio* rate constants involved in this process

$$\text{H-Si-Si-H}_{(a)} \underset{k_{-1}}{\overset{k_1}{\rightleftharpoons}} \text{bare Si} + \text{SiH}_{2(a)} \xrightarrow{k_2} \text{H}_{2(g)} + \text{Si dimer}$$

to be $k_1=4.8\times10^{1}$ s^{-1}, $k_{-1}=2.0\times10^{7}$ s^{-1}, and $k_2=1.4\times10^{-2}$ s^{-1}. Since the forward (k_1) and reverse (k_{-1}) isomerization processes happen so much faster than the desorption process ($\tau_1=1\times10^{-2}$ s, $\tau_{-1}=1\times10^{-8}$ s, and $\tau_2=7\times10^{1}$ s), a preequilibrium, which is dramatically tilted in favor of monohydride creation, is established between the monohydride and dihydride isomers.

In summary (refer to the first and second columns of Table I), we have determined a dynamical hierarchy of events in which defect migration, parallel diffusion, and dihydride to monohydride isomerization are extraordinarily fast; defect-induced isomerization (both forward and backward) is rapid; monohydride to dihydride isomerization occurs at a moderate rate; and perpendicular diffusion and desorption are rare events. The remaining task is to place these processes into a KMC scheme.

C. Kinetic Monte Carlo applied to hydrogen desorption from Si(100)−2×1

An ideal model would include all of these processes regardless of whether or not the anticipated effect on the kinetics of desorption was significant. However, because in a KMC simulation we choose one process to be the reference, i.e., the process by which the occurrence of all other events is determined and from which the time is updated, to keep the KMC simulation computationally feasible (as explained in Sec. II A), it is necessary to choose to simulate events that are not on dramatically different time scales.

The extremely rapid events, parallel diffusion and defect migration, happen so rapidly compared to the other processes, that it seems that the result of these rapid events is to make the distribution of hydrogen atoms and defects appear random to processes which occur on longer time scales. Thus, we feel that it is reasonable to model these very fast events as randomizing processes which we include in full at every step of the simulation. For defect migration, this means that before any other type of event is attempted each lone silicon is given a chance, on the flip of a coin, to isomerize with any neighboring, bare silicon dimers. Since our simulation assumes that adsorbate hydrogen atoms are prepaired on silicon dimers, the effect of parallel diffusion in our model is to randomize the monohydride and bare dimer populations completely before each attempted move. We think that this random mixing step can effectively mimic the rapid populating and depopulating of silicon dimers with adsorbate hydrogen atoms that we anticipate results from the parallel diffusion process. An analysis of the random mixing step is provided in Sec. III E.

We believe that it will not affect the model much to leave out the only remaining very fast process, dihydride to monohydride isomerization, and the reverse process, monohydride to dihydride isomerization which has a moderate rate. Although in a real system there will always be a finite number of dihydrides formed through this isomerization mechanism, we anticipate that the overall effect on the desorption rate will be small as the number of dihydrides formed is predicted to be minuscule.

Similarly, we elect to leave out hydrogen atom diffusion perpendicular to the silicon dimer rows. Since the rate constant of this process is predicted to be slower than hydrogen desorption, it is doubtful that it will significantly influence the overall kinetics.

All of these events, besides hydrogen diffusion parallel to the silicon dimer rows (parallel diffusion), can be simulated by constructing a one-dimensional (1D) chain of dimers run-

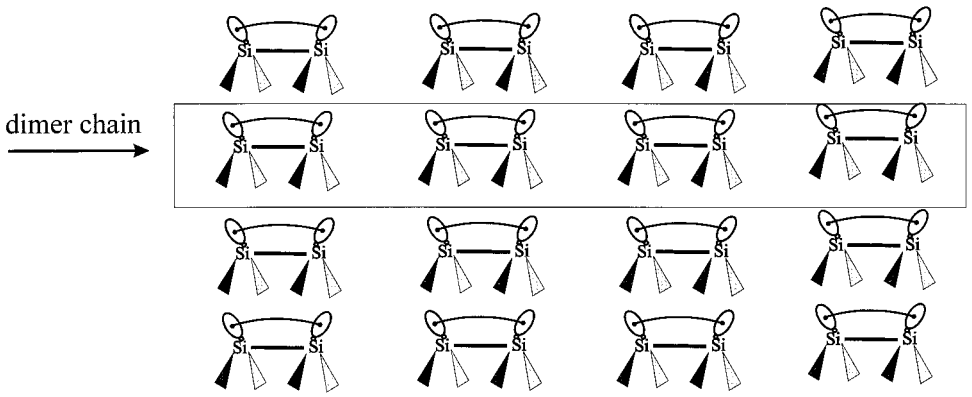

FIG. 1. The dimer chain used in the simulations is composed of dimers running perpendicular to the dimer rows on Si(100)-2×1.

ning perpendicular to the dimer rows (Fig. 1). Since we attempt to include the effect of parallel diffusion as a step which randomizes the monohydride population, then we can also include this in a 1D model, simply by randomly mixing the monohydride and bare dimers in this array. Table I gives a summary of these processes and their role in the KMC model.

In our specific implementation of the KMC simulation, then, we explicitly include the rate constants for defect-induced conversion of monohydrides to dihydrides (forward and reverse) and hydrogen desorption from the dihydride. Since we calculated the rate constant for forward isomerization to be the quickest, this is the reference rate constant, k_r. We implicitly include defect migration and parallel diffusion by randomizing the defect, monohydride, and bare dimer populations before attempting any KMC moves. In step 1, an adsorbate hydrogen atom is chosen at random. Based on the type of adsorbate selected (monohydride or dihydride), in step 2, a direction for a move is randomly picked, either to a neighboring side for a defect-induced isomerization/reverse isomerization process or desorption (only in the case of a dihydride being picked in step 1). For step 3, the neighbor of the chosen adsorbate is analyzed to see which type of processes can occur. If the atom picked is a monohydride and the selected direction is toward a neighboring, empty defect, dihydride isomerization might occur. Likewise, if the atom picked is a dihydride and the chosen direction is toward a bare silicon dimer, then reverse isomerization to a monohydride might happen. Or for a dihydride, desorption can be the selected direction. If the event chosen in step 3 is possible, it occurs with a probability of k/k_r in step 4. Otherwise, the move is aborted. After each attempted move, the defect and monohydride populations are randomized again and the simulation loops through the above steps once more. After N attempted moves, where N is the number of adsorbate hydrogen atoms present at the beginning of the loop, the time is incremented by $1/k_r$. N is reset after each loop to reflect a possibly reduced number of adsorbate hydrogen atoms.

D. Data analysis

To ascertain the kinetic order our model predicts for hydrogen desorption under a variety of different conditions, we look at the equations for first-order $[d\theta_H/dt=-k\theta_H]$ and second-order $[d\theta_H/dt=-k\theta_H^2]$ kinetics, with respect to hydrogen coverage (θ_H). From these equations, it is obvious that $-\ln(\theta_t/\theta_{t=0})$ plotted against time should be a straight line if the kinetics are first order and that $1/\theta_t$ versus time should be a straight line for second-order kinetics. Thus, for each simulation run under different conditions, we analyze our coverage versus time data by plotting it according to the equations above. Additionally, for coverages of 0.25 ML and less, we plot the data according to superlinear $[d\theta_H/dt=-k\theta_H^{1.5}]$ kinetics, under which $1/\sqrt{\theta_t}$ versus time should be a straight line. We do this for the low coverage systems, since Höfer, Li and Heinz,[4] have reported that the kinetic order for hydrogen desorption below 0.1 ML is between first and second order.

To determine the predicted rate constant from the kinetic plots, we use linear least-squares regression with a confidence level of 95%. If the value of the square of the correlation coefficients (R^2) from the line fit is less than 0.95, then we average the results from independent simulations together until R^2 has a value of at least 0.95. This enables us to get better statistics for the kinetic order plots, and is especially important for runs performed on smaller arrays, where there are less hydrogen desorption events to monitor.

III. RESULTS AND DISCUSSION

A. Effect of system size and edge effects

The 1D array of silicon dimers represents a chain of silicon dimers which run perpendicular to the silicon dimer rows on Si(100)-2×1. To test the effect of system size on the model, we performed simulations with varying sizes of arrays using periodic boundary conditions (PBC's) to eliminate the effect of edges. For a system with an initial hydrogen coverage of 0.9 ML and with 10% isolated atom defects at the peak desorption temperature of 800 K, we found that there was no difference in kinetic order or rate constant determined from simulations using 100 (50 silicon dimers, ~400 Å) or 200 atoms (100 silicon dimers, ~800 Å). The kinetic plot in Fig. 2 for the 200 atom system is representative of the overall kinetic order we see for all other systems. Both the 200 and 100 atom systems show the requisite first-order kinetics for hydrogen desorption from Si(100)-2×1 and predict similar rate constants (0.016 s^{-1} for 100 atoms and 0.011 s^{-1} for 200 atoms). Therefore, to keep our computations manageable, we chose to perform the bulk of simulations in this work using 100 atom chains of dimers.

The length of the dimer chain, however, will depend on the morphology of a hydrogen-covered Si(100)-2×1 surface near the temperature at which hydrogen desorption occurs,

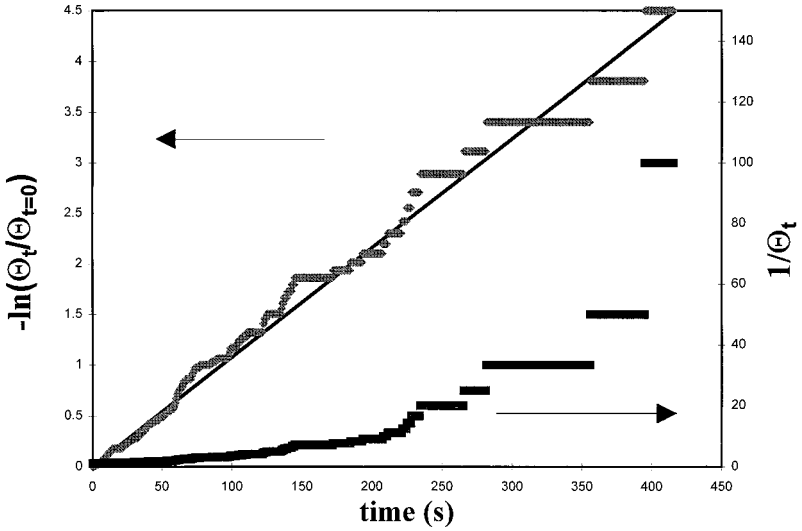

FIG. 2. Hydrogen coverage versus time for a kinetic Monte Carlo (KMC) simulation at 800 K of 200 atoms with periodic boundary conditions and a defect concentration of 10%. The data is plotted according to first-order (left axis) or second-order (right axis) kinetics. The solid line is a linear-least-squares line fit to the first-order kinetic plot. This plot is representative of the first-order kinetics we observe in all our simulations.

and so the effect of surface features which limit the chain length and introduce edges must also be considered. The topology of vicinal Si(100)-2×1 surfaces depends on both the misorientation of the surface from the [100] direction and the temperature. Step density and surface roughness dramatically increase at temperatures above 1300 K,[28] but the desorption experiments circa 800 K are well below this temperature. Thus, it appears that the step density on these surfaces is primarily a result of the miscut of the surface.

Most experiments done on the hydrogen adsorption and desorption report a miscut of less than 0.5°.[4,5,29,30] Monoatomic steps dominate at miscut angles less than 1°,[31] thus, these surfaces can be characterized as having minimum terrace widths of ~150 Å with both S_B [steps which have edges parallel (perpendicular) to dimer rows on the lower (upper) terrace] and S_A steps [steps which have edges perpendicular (parallel) to dimer rows on the lower (upper) terrace]. Depending on the type of terrace they inhabit, chains of dimers perpendicular to the dimer rows can either extend the length of the step edge or the width of the terrace, in either case on the order of hundreds of Å's. On the other hand, dimer chains could be ended by other surface features such as dimer vacancy defects which are prevalent on the surface.[32] To determine the effect of finite dimer chains with edges, we performed several simulations of different sizes without PBC's, i.e., with edges present.

These simulations consisted of dimer chains of 100 (~400 Å), 40 (~150 Å), and 20 (~75 Å) silicon atoms. All of these runs started from 0.9 ML and included 10% defects. The defect concentration of 10% was chosen so that there would be two defects in the 20 atom array, as our model, being based on the prepairing assumption, requires an even number of total atoms and defects. All of these different cell sizes exhibited first-order kinetics, with the rate constant at 800 K determined as $k=0.015$, 0.019, and 0.023 s^{-1}, for the 100, 40, and 20 atoms arrays, respectively. The first-order kinetics are essentially the same as those calculated using PBC's ($k=0.016$, 0.018, 0.017 s^{-1}). However, in the simulations where edges are present there is a slight increase in the rate constant as the cell size decreases. Perhaps, as the dimer chain gets smaller, encounters between defects and monohydrides become more frequent, leading to the creation of more dihydrides.

Since defects might be formed at step edges, we would like to gauge the effect of the initial distribution of defects within a cell without PBC's. We can isolate this effect by comparing a simulation which has defects that start at the boundary of the cell with one run under the same conditions, but in which the initial distribution of defects is random. Because the 40 atom array (~150 Å) represents the approximate width of the terraces in the hydrogen desorption experiments, we make our comparisons using this length of dimer chain. We use a starting coverage of 0.9 ML and include 5% defects (or two defects). When these defects are placed randomly among the dimer chain, we obtain a rate constant of 0.009 s^{-1} compared to a rate constant of 0.008 s^{-1} when the defects are initially placed at a boundary.

In summary, it appears that system size, edge effects, and initial defect distribution have little or no effect on the overall kinetic order and rate constant in our model. However, we see that as the cell size decreases, there is a small increase in the rate constant in systems with edges, due, perhaps, to the presence of ''trapped'' isolated atom defects that may lead to enhanced defect-induced isomerization, followed by desorption. This last result seems to indicate a dependence of the rate constant on the quality of the surfaces, as discussed later.

B. Effect of defect concentration on kinetics

On the other hand, we find that the concentration of defects has a significant impact on the rate constant of hydrogen desorption, although it does not alter the kinetic order. To quantify the impact on rate constant, we performed simulations on a 100 atom array, where the initial concentrations of defects were 10%, 4%, and 2%. These calculations were done at 800 K with an initial hydrogen coverage of 0.9 ML. For 10%, 4%, and 2% defects, our model predicts rate constants which linearly decrease with defect concentration ($k=0.016$, 0.008, and $k=0.004$ s^{-1}, respectively). This result suggests, again, that the quality of Si(100)-2×1 surfaces used in hydrogen desorption experiments affects the rate constant, perhaps explaining the wide range (0.048–2.77 s^{-1}) (Refs. 1–5) of experimentally determined rate constants.

C. Coverage dependence of kinetics

Experimentalists observe that above $\Theta(H)=0.1$ ML, the kinetics of hydrogen desorption are invariant with initial hy-

drogen coverage.[1,4,5] To see whether our model is consistent with these observations, we performed KMC simulations using initial hydrogen coverages of 0.9, 0.24, 0.1, and 0.04 ML's. We chose to include the lowest possible amount of defects, 2%, since room-temperature scanning tunneling microscopy (STM) data[31] suggests this is probably more realistic than a higher percentage. Using a 100 atom cell at 800 K, we find the rate constant at 0.9 ML ($k=0.004$ s^{-1}), 0.24 ML ($k=0.005$ s^{-1}), 0.1 ML ($k=0.004$ s^{-1}), and 0.04 ML ($k=0.004$ s^{-1}). Thus, we see that within our model, the rate constant is invariant with coverage, in agreement with experimental results.

Furthermore, first-order kinetics are followed for all coverages, even low coverages (0.1 and 0.04 ML). This supports the supposition of Höfer, Li, and Heinz[4] that the super first-order kinetics they observed at coverages lower than 0.1 ML is due to a lack of prepairing. Since our model implicitly includes prepairing, we do not see a breakdown in the first-order kinetics at low coverages.

D. Temperature dependence of kinetics

Another condition which leads to an increase in desorption rate, is, as expected, rising temperature. We performed simulations of 100 atoms with 2% and 10% defects and an initial hydrogen coverage of 0.9 ML. As the temperature is raised from 800 to 850 to 900 K, the rate constant changes from $k=0.004$ to 0.033 to 0.195 s^{-1} for simulations with 2% defects and $k=0.016$ to 0.112 to 0.975 s^{-1} for those with 10% defects. Using these values in an Arrhenius plot [$\ln(k)$ versus $1/T$ from the Arrhenius equation $k=Ae^{-E_a/kT}$] yields parameters of $A=1.9\times10^{13}$ s^{-1} and $E_a=2.43$ eV for simulations with 2% defects and $A=1.8\times10^{14}$ s^{-1} and $E_a=2.55$ eV for those with 10% defects. The rate constants calculated from these parameters ($k=0.004$ and 0.015 s^{-1}, for 2% and 10% defects at 800 K, respectively) are nearly identical to those obtained directly from the KMC simulations, i.e., from the slopes of $-\ln\Theta_t/\Theta_{t=0}$ versus time plots ($k=0.004$ and 0.016 s^{-1}, for 2% and 10% defects at 800 K, respectively), as they should be. On the other hand, the experimentally determined rate constant for desorption, which we incorporated into our model as the rate constant for desorption from a dihydride, is 0.196 s^{-1} at 800 K. How this discrepancy can be understood is the subject of the next section.

Upon inspection of the experimentally determined Arrhenius parameters for desorption ($A=1.0\times10^{15}$ s^{-1} and $E_a=2.49$ eV), we see that the activation energies our Arrhenius analysis predicts for simulations with either 2% or 10% defects are in agreement with the experimental activation barrier for desorption. However, the preexponentials for the overall desorption rate constant predicted from our simulations are lower than the prefactor we entered into our model for the desorption step. In fact, we see that the lowest value of the prefactor that we obtain is when there are the least amount of isolated atom defects on the surface. Thus, the overall desorption rate constant depends on the barrier to desorption from the isolated dihydride and not on any preceding steps, while the prefactor depends on the concentration of defects which can form this species. We can understand the reduction in the overall preexponential for desorption due to a decrease in the concentration of defects by recalling that the preexponential represents a ''collision frequency.'' As the number of defects decrease, encounters between defects and monohydrides (essential in forming the dihydride species from which desorption occurs) are more rare, and accordingly, the rate constant is diminished. This results further underlines the effect defect concentration has on the desorption rate constant that we saw in Sec. III B.

E. Examination of errors in the model

We are interested in why our KMC predictions of rate constants for desorption (0.016 s^{-1} for a simulation of 100 atoms with 10% defects at 800 K) are smaller than the experimentally determined value (0.196 s^{-1} at 800 K), even when a large fraction of defects are included in the simulations. The KMC model depends on having good estimates of the relationships of rate constants, k/k_r, something we have attempted to provide but might have made errors in assessing. Therefore, we desire to determine whether our model would predict the same kinetics if the ratios of our calculated rate constants were in error. To test how varying the ratio of the desorption rate to the reference rate changes the model, we added 0.2 eV and then 0.4 eV to the activation barriers for forward and reverse defect-induced isomerization, while leaving the barrier for desorption alone. Decreasing the rate constant for both the forward and reverse defect-induced isomerization processes keeps the relative population of dihydrides to monohydrides the same, but the lifetime of these species is increased. We found, that for a simulation of 100 atoms with 10% defects at 800 K, adding 0.2 eV leads to first-order kinetics with a rate constant of 0.016 s^{-1}, while adding 0.4 eV leads to first-order kinetics with a rate constant of 0.015 s^{-1}. Comparing these kinetics to those of the unaltered system (0.016 s^{-1}), we see that *wide variations in the lifetime of the dihydride species, which is the precursor to desorption in this model, do not affect the predicted kinetics*.

On the other hand, if we vary the population ratio of monohydrides to dihydrides in the simulation (by increasing or decreasing the rate constant of forward isomerization relative to reverse isomerization), we might expect the rate constant to change proportionally with the increase or decrease in dihydride population. Indeed, when we increased the rate constant for the creation of dihydrides (forward isomerization) relative to the rate constant for the destruction of dihydrides (reverse isomerization) by adding 0.2 eV to the activation barrier for reverse isomerization we find that the rate constant increases to 0.038 s^{-1} from 0.016 s^{-1}. *This suggests that any process we might have left out which increases the dihydride population or contributes to the formation of dihydrides could alter significantly our predicted rate constant.*

We also wanted to look at how our treatment of intra-row hydrogen atom diffusion might affect the simulations. To get an idea of how our attempt to include this process through randomizing the monohydride population affects the overall model, we performed some simulations where we left the randomizing step out. Comparing simulations on 100 atoms with 10% defects and initial hydrogen coverages of 0.9 ML and 0.24 ML at 800 K, with and without the random mixing process, we found that both types of simulations predict first-order kinetics. Moreover, we found little difference between the predicted rate constants at either high coverages (k

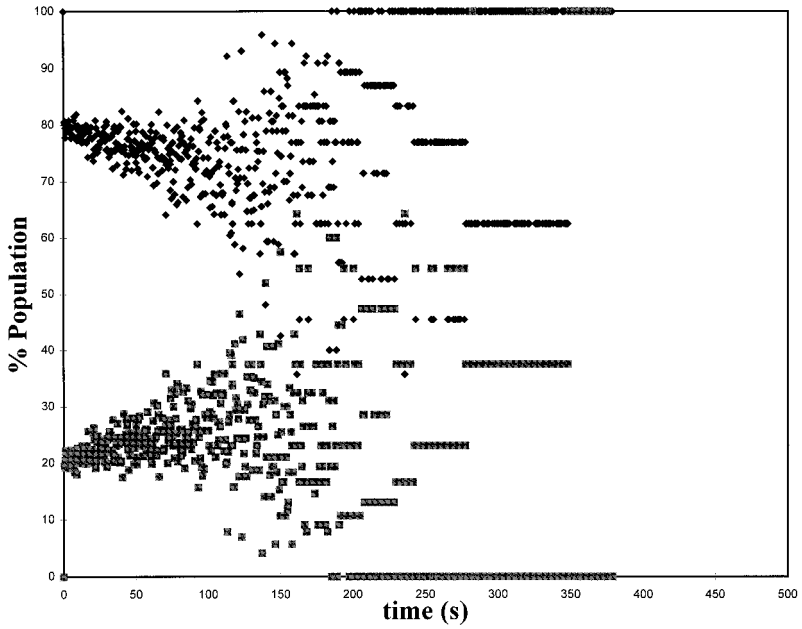

FIG. 3. The population of hydrogen atoms in the monohydride (black diamonds) and dihydride (gray squares) states versus time for a simulation at 800 K of 100 atoms with periodic boundary conditions and a defect concentration of 10% *with* the random mixing step.

$=0.016\ s^{-1}$ for random mixing versus $k=0.011\ s^{-1}$ without) or low coverages ($k=0.019\ s^{-1}$ with or without random mixing).

When we looked at how the percentages of monohydrides and dihydrides changed with time, however, we saw that for the random mixing model the percentage of dihydride species on the surface was consistently higher in the beginning of a 0.9-ML simulation (Fig. 3), while for the simulations without random mixing the percentage was lower (Fig. 4). We reason that random mixing produces a more stable dihydride population initially, because the bare dimer produced in the forward step in the reaction below

$$\text{H-Si-Si-H}_{(a)} + \text{Si} \underset{k_{-1}}{\overset{k_1}{\rightleftharpoons}} \text{SiH}_{2(a)} + \text{Si-Si}$$

might be swept away (through our parallel diffusion process which randomizes the monohydride and bare dimer populations) before the reverse step can destroy the dihydride. As the simulation progresses, the hydrogen coverage becomes smaller and randomly distributing the monohydrides between simulation steps does not affect the system much, since the distribution is already random. Thus, the effect of this process on the rate constant seems to be small or negligible, depending on the initial hydrogen coverage.

That our model predicts an overall rate constant for hydrogen desorption which is smaller than the experimental value which we input initially shows that we could be oversimplifying the effects of defect migration and parallel diffusion and leaving out important pathways on the surface, some of which may be involved in defect creation. The simplifications in our model are necessitated by our lack of complete knowledge of all surface processes involving hydrogen

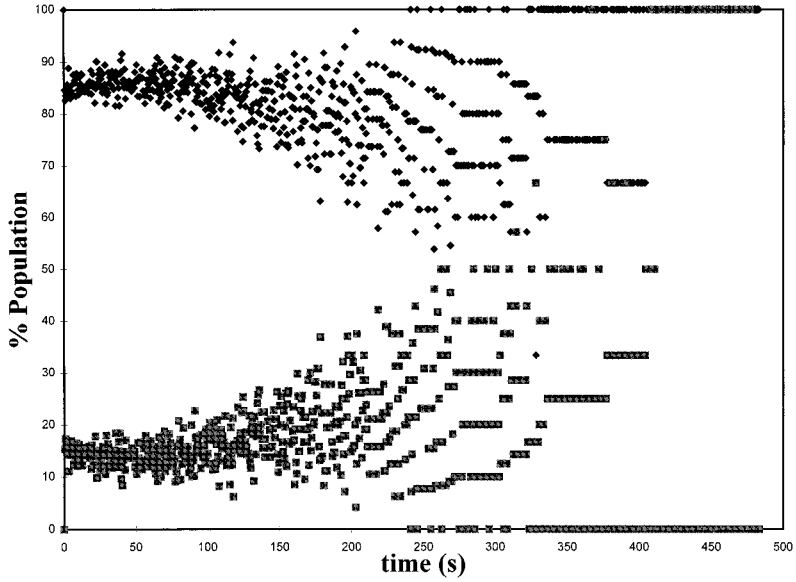

FIG. 4. The population of hydrogen atoms in the monohydride (black diamonds) and dihydride (gray squares) states versus time for a simulation at 800 K of 100 atoms with periodic boundary conditions and a defect concentration of 10% *without* the random mixing step.

on Si(100)-2×1, surface topology, and a desire to keep the simulations computationally feasible. Many rate constants are not known for defect creation from steps or for parallel and perpendicular hydrogen atom diffusion to defect sites or to silicon atoms with one hydrogen already present, processes which could affect the overall kinetics. We have provided reasons for the approximations we have made, but pathways we have overlooked may contribute to the hydrogen desorption process, and may explain why our predicted rate constant is lower than experimentally determined values. For instance, we saw in Sec. III A that as the size of the dimer chain is reduced, edge effects play a role in increasing the rate constant. On a real surface, dimer vacancies and steps are numerous, and both of these features could serve to limit the dimer chain size, enhancing the rate constant for desorption.

We saw, above, that increasing the population of dihydrides present on the surface effectively doubled the rate constant, implying that any mechanism which would serve to create more dihydrides would increase the rate constant. One possibility for creating more dihydrides is the monohydride-dihydride single dimer isomerization mechanism which converts monohydrides to dihydrides. We left this mechanism out of our model, arguing that a significant dihydride population is not produced through this mechanism since the rate constant for reversion to the monohydride ($k_{\text{reverse}}=2.0\times10^{7}\ \text{s}^{-1}$) is much faster than the rate constant for dihydride production ($k_{\text{forward}}=4.8\times10^{1}\ \text{s}^{-1}$). However, if defect migration, which we estimate to have a rate constant between 10^{6} to $10^{11}\ \text{s}^{-1}$, is faster than the rate constant for dihydride reversion, the bare silicon next to the isolated dihydride might migrate away before the monohydride can be reformed:

$$\text{H-Si-Si-H}_{(a)}+\text{Si-Si}\underset{k_{-1}}{\overset{k_1}{\rightleftharpoons}}\text{SiH}_{2(a)}+\text{bare Si}\qquad \text{Si}+\text{Si-Si}\underset{k_{-2}}{\overset{k_2}{\rightleftharpoons}}\text{SiH}_{2(a)}$$

$$+\text{Si-Si}+\text{bare Si}.$$

This latter mechanism could also lead to an increased desorption rate constant, since it would increase the average population of dihydrides on the surface.

IV. CONCLUSIONS

Based on this model, we conclude that the isolated dihydride mechanism follows first-order kinetics within the framework of a mechanism where dihydrides are systematically created from monohydrides. We find that first-order kinetics are predicted regardless of system size, edge effects, defect concentration, hydrogen coverage, and temperature. Furthermore, we find that the rate constant has little or no dependence on all of these factors except for defect concentration and temperature. The independence of the rate constant and kinetic order on coverage is in agreement with experiments which look at hydrogen coverages above 0.1 ML. Below this coverage, the predictions of our model run contrary to experimental results which show a supralinear kinetic order,[4] perhaps indicating that the prepairing assumption, which is inherent in our model, breaks down at very low coverages. It makes sense, physically, that prepairing should not be automatic at very low coverages, since it will take much longer for the hydrogen atoms to find each other. In such a circumstance, random diffusion may be more characteristic of the events that form the dihydride, leading to an increase in the kinetic order.

On the other hand, our prediction that the rate constant varies with the percentage of defects on the surface, might explain the several order of magnitude range in experimentally determined measurements of this quantity. We suggest that high temperature (circa 800 K) STM studies of the Si(100)-2×1 and Si(100)-2×1:1H surfaces might shed some light on the role of defects in hydrogen desorption. As far as we know, there have been no attempts to characterize the Si(100)-2×1 surface, investigating types and concentrations of defects, near the hydrogen desorption temperature. (We realize that this is a nontrivial experiment.) Instead, STM data on defects on this surface have been limited to room temperature. Our prediction that the rate constant for desorption is influenced by defect concentration might be tested experimentally by hydrogen desorption studies from surfaces which have been rigorously characterized. If step edges are a source of defects, as Jing, Lucovsky, and Whitten[17] have suggested, surfaces with a higher miscut angle (resulting in higher step densities) should yield higher rate constants for desorption.

ACKNOWLEDGMENTS

We wish to acknowledge the late Professor Brian Bent, with whom E.A.C. had stimulating discussions about the unusual kinetic order in this system. This work was primarily supported by the Air Force Office of Scientific Research. We are grateful to Professor Ken Jordan for providing optimized geometries for the defect isomerization and defect migration mechanisms and to Dr. Zhenyu Zhang for helpful discussions on KMC simulations. E.A.C. also acknowledges the Camille and Henry Dreyfus Foundation and the Alfred P. Sloan Foundation for support.

*To whom correspondence should be addressed.

[1] K. Sinniah, M. G. Sherman, L. B. Lewis, W. H. Weinberg, J. T. Yates, Jr., and K. C. Janda, J. Chem. Phys. **92**, 5700 (1990).
[2] M. L. Wise, B. G. Koehler, P. Gupta, P. A. Coon, and S. M. George, Surf. Sci. **258**, 5482 (1991).
[3] K. Sinniah, M. G. Sherman, L. B. Lewis, W. H. Weinberg, J. T. Yates, Jr., and K. C. Janda, Phys. Rev. Lett. **62,** 567 (1989).
[4] U. Höfer, L. Li, and T. F. Heinz, Phys. Rev. B **45**, 9485 (1992).
[5] M. C. Flowers, N. B. H. Jonathan, Y. Liu, and A. Morris, J. Chem. Phys. **99**, 7038 (1993).
[6] For a more thorough review of theoretical and experimental work on this topic see M. R. Radeke and E. A. Carter, Phys. Rev. B **54**, 11 803 (1996).
[7] M. R. Radeke and E. A. Carter, Surf. Sci. **355**, L289 (1996): Phys. Rev. B **54**, 11 803 (1996).
[8] C. J. Wu, I. V. Ionova, and E. A. Carter, Surf. Sci. **295**, 64 (1993).
[9] P. Nachtigall, K. D. Jordan, and K. C. Janda, J. Chem. Phys. **95**, 8652 (1991).
[10] C. J. Wu and E. A. Carter, Chem. Phys. Lett. **185**, 172 (1991).
[11] M. P. D'Evelyn, Y. L. Yang, and L. F. Sutcu, J. Chem Phys. **96**, 852 (1992).

[12] J. J. Boland, Phys. Rev. Lett. **67**, 1539 (1991); J. Vac. Sci. Technol. A **10**, 2458 (1992).
[13] Y. L. Yang and M. P. D'Evelyn, J. Vac. Sci. Technol. A **11**, 2200 (1993).
[14] P. Nachtigall, K. D. Jordan, and C. Sosa, J. Chem. Phys. **101**, 8073 (1994).
[15] Z. Jing and J. L. Whitten, J. Chem. Phys. **102**, 3867 (1995).
[16] A. C. Luntz and P. Kratzer, J. Chem. Phys. **104**, 3075 (1996).
[17] Z. Jing, G. Lucovsky, and J. L. Whitten, Surf. Sci. Lett. **296**, L33 (1993).
[18] K. W. Kolasinski, W. Nessler, A. de Meijere, and E. Hasselbrink, Phys. Rev. Lett. **72**, 1356 (1994); K. W. Kolasinski, W. Nessler, K.-H. Bornscheuer, and E. Hasselbrink, Surf. Sci. **331**, 485 (1995).
[19] K. W. Kolasinski, W. Nessler, K.-H. Bornscheuer, and E. Hasselbrink, J. Chem. Phys. **101**, 7082 (1994).
[20] K. A. Fichthorn and W. H. Weinberg, J. Chem. Phys. **95**, 1090 (1991).
[21] Y.-T. Lu and H. Metiu, Surf. Sci. **245**, 150 (1991).
[22] Nachtigall *et al.* defined the pathway for this reaction as going through a local minimum, LM (H-Si-Si-$H_{(a)}$+Si $-$TS1$\rightarrow$ LM $-$TS2$\rightarrow$ $SiH_{2(a)}$+Si-Si). As this local minimum is less than 0.05 eV below the first transition state, we treat this reaction as a one-step process and use the overall reaction barriers in our model.
[23] All HFSCF calculations were performed using the program HONDO. M. Dupuis, A. Marquez, and E. R. Davidson, ''HONDO 95.3 from CHEM-Station,'' IBM Corporation, Neighborhood Road, Kingston, NY (1995).
[24] This basis set is the first contracted *s* function in the 3-21 G basis set for H from J. S. Binkley, J. A. Pople, and W. J. Hehre, J. Am. Chem. Soc. **102**, 939 (1980).
[25] J. I. Steinfield, J. S. Francisco, and W. L. Hase, *Chemical Kinetics and Dynamics* (Prentice Hall, Englewood Cliffs, New Jersey, 1989).
[26] C. J. Wu, J. V. Ionova, and E. A. Carter, Phys. Rev. B **49**, 13 488 (1994); C. J. Wu and E. A. Carter, *ibid.* **46**, 4651 (1992).
[27] A. Vittadini, A. Selloni, and M. Casarin, Surf. Sci. Lett. **289**, L625 (1993).
[28] See R. J. Hamers, R. M. Tromp, and J. E. Demuth, Phys. Rev. B **34**, 5343 (1986), and references therein.
[29] P. Bratu, K. L. Kompa, and U. Höfer, Chem. Phys. Lett. **251**, 1 (1996).
[30] K. W. Kolasinski, W. Nessler, K.-H. Bornscheuer, and E. Hasselbrink, J. Chem. Phys. **101**, 7082 (1994).
[31] See, for example, M. G. Lagally, Y. W. Mo, R. Kariotis, B. S. Swartzentruber, and M. B. Web., in *Kinetics of Ordering and Growth at Surfaces* (Plenum, New York, 1990).
[32] R. J. Hamers. R. M. Tromp and J. E. Demuth, Phys. Rev. B **34**, 5343 (1986); Ph. Avouris and D. Cahill, Ultramicroscopy **42–44**, 838 (1992).